Spherical Mechanism Analysis of a Surgical Robot for Minimally Invasive Surgery – Analytical and Experimental Approaches

Jacob Rosen[1,2], Ph.D., Mitch Lum[1] BSEE., Denny Trimble[3] , BSME
Blake Hannaford[1,2], Ph.D., Mika Sinanan[2,1] , M.D., Ph.D.

[1] Department of Electrical Engineering, [2] Department of Surgery, [3] Department of Mechanical Engineering,
University of Washington, Seattle, WA, USA
E-mail: <rosen, mitchlum, mssurg, blake>@u.washington.edu>
Biorobotics Lab: http://brl.ee.washington.edu
Center of Videoendoscopic Surgery: http://depts.washington.edu/cves/

Abstract: Recent advances in technology have led to the fusion of MIS techniques and robot devices. However, current systems are large and cumbersome. Optimizing the surgical robot mechanism will eventually lead to its integration into the operating room (OR) of the future becoming the extended presence of the surgeon and nurses in a room occupied by the patient alone. By optimizing a spherical mechanism using data collected *in-vivo* during MIS procedures, this study is focused on a bottom-up approach to developing a new class of surgical robotic arms while maximizing their performance and minimizing their size. The spherical mechanism is a rotational manipulator with all axes intersecting at the center of the sphere. Locating the rotation center of the mechanism at the MIS port makes this class of mechanism a suitable candidate for the first two links of a surgical robot for MIS. The required dexterous workspace (DWS) is defined as the region in which 95% of the tool motions are contained based on *in-vivo* measurements. The extended dexterous workspace (EDWS) is defined as the entire abdominal cavity reachable by a MIS instruments. The DWS is defined by a right circular cone with a vertex angle of 60º and the EDWS is defined by a cone with an elliptical cross section created by two orthogonal vertex angles of 60º and 90º. A compound function based on the mechanism's isotropy and the mechanism stiffness was considered as the performance metric cost function. Optimization across both the DWS and the EDWS lead to a serial mechanism configuration with link length angles of 74º and 60º for a serial configuration This mechanism configuration maximized the kinematic performance in the DWS while keeping the EDWS as its reachable workspace. Surgeons, using a mockup of two mechanisms in a MIS setup, validated these results experimentally. From these experiments the serial configuration was deemed most applicable for MIS robotic applications compared to a parallel mechanism configuration. The mechanical design of a cable actuated surgical robot was based on optimized link length angles. The system is currently being integrated into a fully operated two-arm system. Small form-factor surgical robotic arms with optimized dexterous workspaces will facilitate the integration of multiple arms while avoiding self-collision in the OR of the future.

1. INTRODUCTION

The OR of the future has been envisioned as a space that will contain only one human being - the patient [1] the presence of surgeons and nurses will be replaced by enabling technologies such as surgical robots, tool changers, equipment dispensers and imaging modalities. Pioneering work in the field of surgical robotics demonstrates that the surgeon can be safely removed from the immediate surgical scene and maintain interaction with the patient in a teleoperational mode [2-5, for review see 6,7]. Duplicating the presence of two surgeons would require at least four highly dexterous surgical robotic arms. Using four robotic arms will clutter the limited space above the patient, while exposing the arms to possible self-collision and limit access to internal anatomy. The scope of this study is to optimize the mechanism of a spherical serial mechanism based on a measured workspace database acquired during MIS setup [8] and to assess its performance.

2. TOOLS AND METHODS

2.1 Spherical Serial Mechanism - Analytical Analysis

The mechanism under study is a member of a class of spherical mechanisms in which all the links' rotation axes intersect in a signal point located at the center of the mechanism. Aligning this point with the location of the port through which tools are inserted into the body in MIS eliminates any tool translation along the orthogonal axes of the tool's shaft. The center of the sphere is the origin for all reference frames of the mechanism. Thus, each link frame is a pure rotation from one to the next.

The coordinate frames are assigned such that the Z-axis of the n'th frame points outward along the nth joint [19]. The numbering scheme for the frames has odd numbers (Frames 0', 1, 3 and 5). The end-effector frame is Frame 5. Frame 0' is oriented such that the z-axis points along joint 1 and the y-axis points to the apex of the sphere. The link angle, α_{i+1} expresses the angle between the ith and $(i+1)$th axis. These are fixed parameters defined by the mechanism geometry. The rotation angle θ_i defines the angle as a function of time between the rotation axis i-1 and i. When all joint angles are set to 0 ($\theta_1=\theta_3=0$), link 13 lies in a plane defined by $Z_{0'}$ and $Y_{0'}$, link 35 is folded back on link 13.

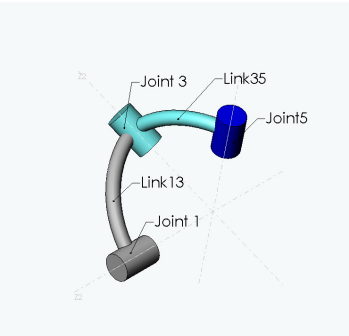

i-1	i	$i+1$	α_{i-1}	θ_i
0'	1	3	0	θ_1
1	3	5	$-\alpha_{13}$	θ_3
3	5	-	α_{35}	$-\theta_5 = 0$

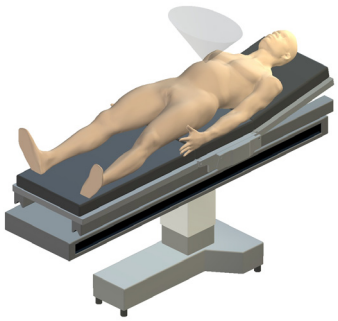

(a) (b) (c)

Figure 1: Spherical serial two link mechanism (a) link and joint assignment based on the Denavit-Hartenberg (DH) notation (b) the mechanism DH parameter notation summary where link number is denoted by i the link length denoted by α_{i-1} ,and the joint angles denoted by θ_i (c)Workspace in Minimally invasive surgery: An elliptical cone with a vertex angle of 60-90 degrees represents the reachable workspace such that any organ in the abdomen can be reached by the endoscopic tool. Note that the azimuth and elevation angles of the cone are free parameters that are determined by the relation between the port location and the targeted organ, (c) The EDWS plotted in one pose with respect to the human body

Analyzing a database collected by the Blue DRAGON [8] of generic surgical tasks including tissue handling/examination, tissue dissection, and suturing performed on an animal model in-vivo by 30 surgeons in a MIS environment indicates that 95% of the time the positions of the surgical tools encompass in a cone with a vertex angle of 60º with a tip located at the port. In addition, measuring the reachable workspace of an endoscopic tool performed on a human model showed that in order to reach any organ in the abdomen the tool needed to move 90º in the lateral/medial direction (left to right) and 60º in the superior/inferior (foot to head) direction (Fig. 1c).

The reachable workspace of the spherical manipulator is a sector of a sphere. The size and the shape of this sector are determined by the mechanism joint lengths (α_{13}, α_{35}), and joint limits. Based on the in-vivo measurements, the dexterous workspace (DWS) for the surgical robot was defined as the area on the sphere bounded by the closed line created when a right circular cone with a circular cross section and a vertex angel of 60º located at the center of the sphere intersected the sphere. The extended dexterous workspace (EDWS) of the surgical robot was defined in a similar fashion; however, the 'cone' had an elliptical cross section created by two orthogonal vertex angels of 60º and 90º. The optimization process aimed to define the mechanism parameters (link lengths) allowing it to reach any point the EDWS and provide high dexterity in the DWS. Based on the mechanical design limits of the mechanism, the range of motion of the first joint angle is 180º ($0º<\theta_1<180º$) and the range of motion of the second joint angle is 160º ($20º<\theta_3<180º$). These constrains were further used to limit the design space from which an optimal solution was searched.

The forward and inverse kinematics of the serial spherical mechanism were developed in [9]. The Jacobian matrix (J) relates joint velocities ($\dot{\theta}_i$) to end-effector angular velocities (ω_i) where ${}^{i+1}_{i}R$ is the rotation matrix expressing the origin of frame $i+1$ in frame i, and $\hat{z}_{i+1}$ is a unit vector along the Z- axis of the $i+1$ frame aligned along the rotational axis. Utilizing the recursive expression for the Jacobian matrix (Eq. 1) [10] along with DH transformation matrices of the mechanism Jacobian can be explicitly expressed in Eq. 2. The eigenvalue corresponding to the angular velocity of Frame 5 has a value of 1 for all poses and joint velocities when the Jacobian matrix is expressed in Frame 5. This allows for the reduction of the Jacobian dimension. The upper 2x2 submatrix of the 3x3 Jacobian matrix is thus used. This truncated version of the Jacobian relates the two controlled joint velocities, 1 and 3 to end-effector velocity. The current analysis uses mechanism isotropy (*ISO*) as the performance metric, defined in Eq. 3 as the ratio between the lowest eigenvalue ($\lambda_{\min}$) and the highest eigenvalue ($\lambda_{\max}$) of the Jacobian matrix. For a given a design candidate (α_{13}, α_{35}), the mechanism isotropy is a function of the joint angles (θ_1, θ_2) and has a value in the range of 0 to 1. An isotropy measure of 0 means the mechanism is in a singular configuration and has lost a degree of freedom. A typical singular configurations of the mechanism under study is obtained when the to links are fully stretched. An isotropy measure of 1 means that the eigenvalues of the Jacobian are all equal and the mechanism can move equally well in all directions.

$$\left[{}^{i+1}\omega_{i+1}\right] = \left[{}^{i+1}_{i}R\right]\left[{}^{i}\omega_{i}\right] + \dot{\theta}^{i+1}_{i+1}\,\hat{z}_{i+1} \tag{1}$$

$$\begin{bmatrix} {}^{5}\omega_{5x} \\ {}^{5}\omega_{5y} \end{bmatrix} = \left[J_5\right]\begin{bmatrix} \dot{\theta}_1 \\ \dot{\theta}_3 \end{bmatrix} = \begin{bmatrix} -Sin\theta_3 Sin\alpha_{35} & 0 \\ -Cos\theta_3 Sin\alpha_{13} Cos\alpha_{35} + Cos\alpha_{13} Sin\alpha_{35} & Sin\alpha_{35} \end{bmatrix}\begin{bmatrix} \dot{\theta}_1 \\ \dot{\theta}_3 \end{bmatrix} \tag{2}$$

$$ISO(\theta_1,\theta_3) = \frac{\lambda_{\min}}{\lambda_{\max}} \qquad ISO \in \langle 0,1 \rangle \tag{3}$$

A scoring function defined in Eq. 4, that is later used as the cost function of the mechanism optimization process, is a compound function that utilizes isotropy measure (Eq. 3) for quantitatively assessing the mechanism performance over its entire designated workspace. The scoring function is a synthesis of three individual elements including (1) an integrated average isotropy measure over the mechanism workspace, (2) a minimal isotropy measure score in the mechanism workspace and (3) the cube of the angular length of the links

$$\phi(\alpha_{13},\alpha_{35}) = \frac{S_{\text{sum}} \cdot S_{\text{min}}}{(\alpha_{13}+\alpha_{35})^3} \qquad (4)$$

In order to analyze the mechanism performance, the hemisphere is discretized into points distributed equally in azimuth and elevation. Given the ranges of the azimuth angle σ and the elevation angle ζ, defining the intersection area between a right circular cross section cone (DWS and EDWS) with a vertex angle of 60º or 90º and located at the center of the sphere and the sphere itself, the set of all possible intersection areas on the hemisphere is $K = \{k(\sigma,\zeta) : 0 < \sigma < 2\pi, 0 < \zeta < \pi/4\}$. The set of all the discrete points contained in the intersection area is $k^p_{\sigma,\zeta} \subset k_{\sigma,\zeta}$. Due to the discrete nature of the computation, each point included in the intersection area has an associated isotropy value *ISO* and sector area *A*. Thus the components of the scoring function (Eq. 4) are defined as follows

$$S_{sum} = \underset{K}{MAX}\left\{\sum_{k^p_{\sigma,\zeta}} ISO(\theta_1,\theta_3)A(\sigma,\zeta)\right\} \qquad \text{(a)} \qquad (5)$$

$$S_{\text{min}} = \underset{K}{MAX}\left\{\underset{k^p_{\sigma,\zeta}}{MIN}(ISO(\theta_1,\theta_3))\right\} \qquad \text{(b)}$$

A requirement of the optimization is that over the DWS or EDWS, the mechanism does not encounter any singularities or workspace boundaries. By multiplying the summed isotropy by the minimum isotropy (Eq. 4), candidates that fail to meet this requirement have a score of zero. By dividing by the cube of the sum of the link angles the score reflects proportionality to the mechanisms stiffness or mass. Thus, over a scan of the potential design space, the peak composite score represents a design with maximum average performance, a guaranteed minimum performance, and maximized stiffness.

The optimization considered all combinations of α_{13}, and α_{35} from 16º to 90º in 2º increments for a total of 1444 design candidates. The hemisphere was discretized into 3600 points, distributed evenly in azimuth and elevation.

$$max\ \phi(\alpha_{13},\alpha_{35}) \begin{cases} 16^o < \alpha_{13} < 90^o \\ 16^o < \alpha_{35} < 90^o \end{cases} \qquad (6)$$

2.2 Spherical Mechanism - Experimental Evaluation

Two re-configurable mockups of both serial and parallel versions of the spherical mechanism were design and fabricated with adjustable link lengths. The human torso was used to assess potential collisions between two surgical arms with different combinations. In addition, the selected configurations were tested in a real MIS setup in which surgical tools were inserted through the apex of the spherical mechanisms. Using real surgical tools, gross tasks such as tissue manipulation as well as high dexterous tasks such as suturing were performed by surgeons while the spherical mechanism following passively the motion

of the tools. Qualitative assessment of range of motion and potential collisions were performed.

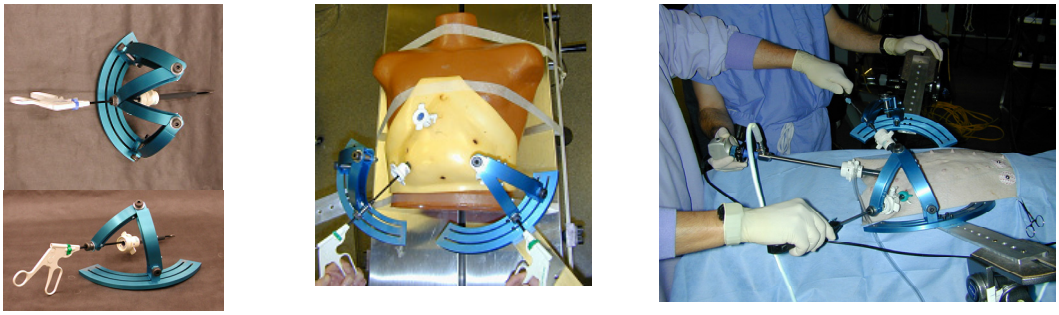

(a) (b) (c)

Figure 2: Experimental setups of the spherical mechanism mock-ups with adjustable link length and base length. The surgical endoscopic tool is inserted into a guide located at mechanism apex in a configuration that allow to test different design candidates in a real MIS setup. (a) Parallel configuration – (top) and serial configuration- (bottom) (b) Two serial configurations tested in a MIS setup with a human torso (c) Two serial configurations tested with an animal model.

3. RESULTS

Optimizing for the DWS, the best design was achieved with link angles of α_{13}=52º and α_{35}=40º (Fig. 2a). In contrast, running the same optimization but requiring a cone with a vertex angle of 90º indicated that the optimal mechanism design has link angles α_{13}=90º and α_{35}=72º (Fig. 2b). The difference in the results is not unexpected but it does pose an interesting dilemma. If one chooses the design that optimizes on a cone with a vertex angle of 90º, the resulting design should be more likely to reach all the poses that manipulator would be asked to reach. However, this design has lower overall performance than the design optimized on for the DWS and larger links, which may increase the likelihood for problems of collisions between two manipulators.

One interesting consideration is to take the best design that is optimized for the DWS that also has the ability to reach a cone with a vertex angle of 90º. This is done by eliminating all the solutions representing mechanism candidates that that cannot reach a cone with a vertex angle of 90º. This optimal design has link angles with α_{13}=72º and α_{35}=60º (Fig. 2c).

Assessing the different combinations of two arms (serial and parallel) in the same surgical scene indicated that two serial mechanisms could be integrated into a MIS surgical scene with minimal potential of self- collision. Setting the adjustable link length angles of the two mockups while manipulating MIS tools through the apex of the mockups indicated that they provided the required workspace needed to complete the surgical tasks under study.

DWS as well as total link length in order to yield a very compact, high-dexterity mechanism. The definitions of the DWS and EDWS were derived based on an experimental database of the kinematics of surgical tools in MIS as collected by the Blue DRAGON system. The optimization results were translated into an actual mechanical design. A further system optimization could include placement of two or more manipulators over a patient while optimizing the individual sub system position and orientations to avoid robot-patient collisions as well as robot-robot collisions and self-collision.

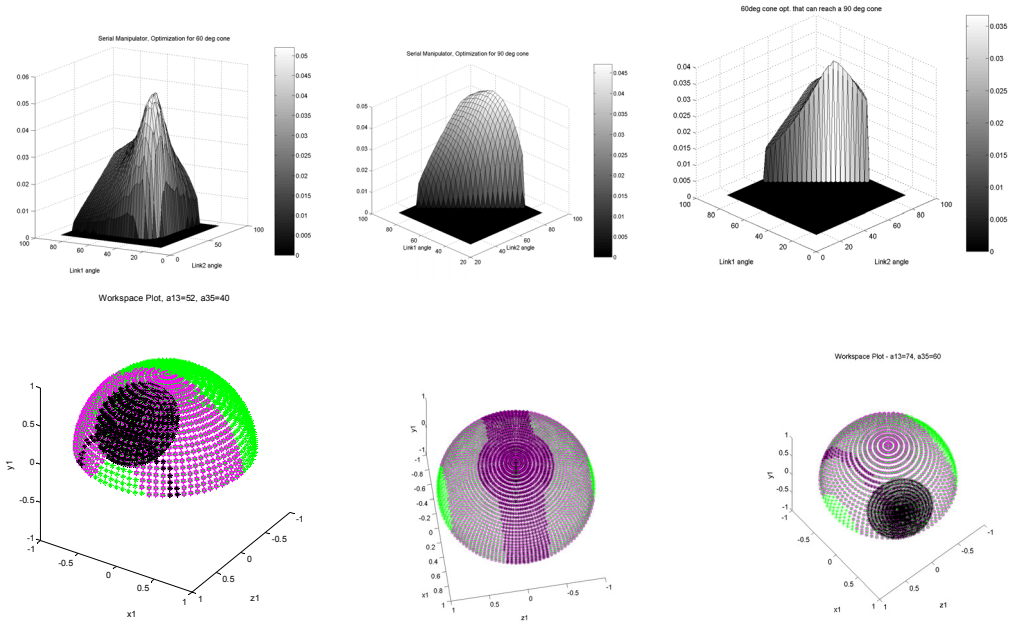

Figure 3: The composite score ϕ of a serial mechanism as a function of the link length angles Link1 (α_{13}), Link2 (α_{35}) along with the workspace of the mechanism with the best performance for each design criterion (peak of a) DWS, a cone with a vertex angle of 60° (b) Workspace plot for optimal mechanism (a) with link angles α_{13}=52° and α_{35}=40° (c) EDWS, a cone with a vertex angle of 90° (d) Workspace plot for optimal mechanism (peak of c) with link angles α_{13}=90° and α_{35}=72°, (e) subset of (a) which can reach a cone with a vertex angle of 90°. (f) Workspace plot for optimal mechanism (peak of e) with link angles α_{13}=74° and α_{35}=60°. For subplots c,d,f, the workspace plots show the hemisphere in green, the reachable workspace in purple, and the orientation of the best cone in black, with the strip of maximum isotropy also in black.

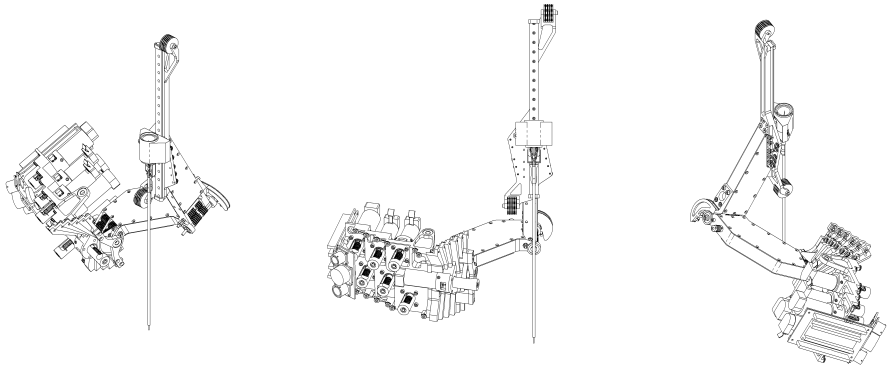

Figure 4: CAD rendering of a serial spherical surgical robotic arm design that was based on link length angles obtained as part of the optimization process under study

4. DISCUSSION

Robotic arms that replace the presence of the surgeon and nurses in the operating room occupy both the space above and inside the patient during both open and MIS setups. These spaces are strictly dictated by the human anatomy. This study provides an optimization methodology for minimizing the size of a spherical surgical robotic arm in

order to avoid potential collisions when more than one arm is introduced into the surgical scene. The optimization balanced a guaranteed minimum and integrated isotropy over the

REFERENCES

[1] Satava, R. Disruptive visions: the operating room of the future, Surgical Endoscopy, 2003, 17(1), 104-107.
[2] Taylor, R.; Lavallee, S.; Burdea, G.; Mosges, R. Computer-Integrated Surgery, MIT Press: Cambridge, MA, 1996.
[3] M.C. Cavusoglu, F. Tendick, M. Cohn, and S.S. Sastry, ``A Laparoscopic Telesurgical Workstation,'' IEEE Trans. Robotics and Automation, vol 15, no. 4, pages 728-739, August 1999.
[4] Madhani, A.; Niemeyer, G.; Salisbury, K. The Black Falcon: A Teleoperated Surgical Instrument for Minimally Invasive Surgery. IEEE/RSJ Int. Conf. on Intelligent Robots and Systems (IROS), Victoria B.C., Canada, October, 1998.
[5] Marescaux, J.; Leroy, J.; Gagner, M.; Rubino, F.; Mutter, D.; Vix, M.; Butner, S.; Smith, M.K. Transatlantic Robot-Assisted Telesurgery, Nature Magazine, 2001, 413, 379-380.
[6] Howe, R.; Matsuoka, Y. Robotics for Surgery. In Annual Review of Biomedical Engineering, 1999, 1, 211 - 240.
[7] J. E. Speich and J. Rosen, Medical Robotics, In Encyclopedia of Biomaterials and Biomedical Engineering, Gary Wnek and Gary Bowlin (Editors), pp. 983-993, Marcel Dekker, Inc, NY, 2004
[8] Rosen, J.; Brown, J.; Chang, L.; Barreca, M.; Sinanan, M.; Hannaford, B. The Blue DRAGON - A System for Measuring the Kinematics and the Dynamics of Minimally Invasive Surgical Tools In–Vivo, Proceedings of the 2002 IEEE International Conference on Robotics & Automation, Washington DC, USA, May 11-15, 2002.
[9] M.J.H. Lum, J. Rosen, M. N. Sinanan, B. Hannaford, Kinematic Optimization of a Spherical Mechanism for a Minimally Invasive Surgical Robot, 2004 IEEE International Conference on Robotics & Automation, pp. 829-834, New-Orleans, USA, April 26-30, 2004
[10] Craig J., Introduction to Robotics Mechanics and Control, Addison, Wesley Logmen, Second Edition, 1989